${}^{9}_{\Lambda}$Li and ${}^{16}_{\Lambda}$N high resolution spectroscopy by electron scattering at Jefferson Lab in Hall A

S. Marrone[1], A. Acha[2], P. Bydzovsky[3], E. Cisbani[4], C.C. Chang[5], F. Cusanno[6], G. De Cataldo[1], R. De Leo[1], C.W. De Jager[7], R.J. Feuerbach[8], S. Frullani[4], F. Garibaldi[4], D.W. Higinbotham[7], M. Iodice[9], B. Kross[7], L. Lagamba[1], J.J. LeRose[7], P. Markowitz[2], E. Nappi[1], R. Michaels[7], B. Reitz[7], J. Segal[5], M. Sotona[3], G.M. Urciuoli[6], B. Wojtsekhowski[7], and C. Zorn[7]

For the Hall A Collaboration

[1] Dipartimento di Fisica and Istituto Nazionale di Fisica Nucleare, Bari, Italy
[2] Florida International University, Miami, FL 33199, USA
[3] Nuclear Physics Institute, Rez near Prague, Czech Republic
[4] Istituto Superiore di Sanitá, Viale Regina Elena 299, 00161 Rome, Italy
[5] University of Maryland, College Park, Maryland 20742, USA
[6] Istituto Nazionale di Fisica Nucleare, Sezione di Roma, Piazzale Aldo Moro 2 00185 Rome, Italy
[7] Thomas Jefferson National Accelerator Facility, Newport News, VA 23606, USA
[8] College of William and Mary, Williamsburg, VA 23187, USA
[9] Istituto Nazionale di Fisica Nucleare Sezione di Roma Tre, Rome, Italy

Abstract. The preliminary results of the ${}^{9}_{\Lambda}$Li and ${}^{16}_{\Lambda}$N spectra obtained by electron scattering experiment in Hall A at Jefferson Lab in the framework of the experiment E94-107 are reported. These hypernuclei are produced bombarding respectively a ^{9}Be and a waterfall target. After a short description of the experimental equipment and of the data analysis procedures, the main characteristics of the measured spectra, as excited levels, energy resolution, and signal to noise ratio are evidenced.

PACS. 21.80.+a Hypernuclei – 25.30.Rw Inelastic electron scattering

1 Introduction

In recent years hypernuclear spectroscopy is living a renaissance mainly due to the experimental studies with electron scattering experiments performed at Jefferson Lab (JLab) in Hall A [1] and Hall C [2–4]. Up to date, previous information on hypernuclei have mainly been obtained by hadron induced reactions like (K^-,π^-) [5], (π^+,K^+) [6] and (stopped K^-,π^-) [7]. For a comprehensive review see reference [8]. These reactions convert a neutron in the nucleus into a Λ, have a reasonable high cross section, i.e. of the order of 10 mb/sr for (K^-,π^-) and 10 μb/sr for (π^+,K^+), but produce hypernuclear spectra with a poor energy resolution ($\geq$ 1.5 MeV FWHM).

In particular, in the (K^-,π^-) reaction there is a magic kaon laboratory momentum at which the recoil hypernucleus is produced with zero momentum. Hence, substitutional states with no orbital angular momentum transfer (ΔL=0) and non-spin-flip states between the neutron and the Λ are preferentially populated. On the other hand, the (π^+,K^+) reaction produces hypernuclei with a large orbital angular momentum transfer ($\Delta L\neq$0) but it is not able to populate spin-flip excited states (ΔS=0). In this case, it has to be noticed that (K^-,π^-) and (π^+,K^+) reactions are able to produce spin-flip states only at high scattering angle where their cross sections are sizeable lower. Finally the electromagnetic and K^- stopped reactions convert a proton into a Λ and therefore give access to different hypernuclei. Moreover the $(e,e'\ K)$ reactions are able to populate unnatural parity spin-flip states ($\Delta S\neq$0), and allow the measurement of hypernuclear spectra with a very good energy resolution (around 650 keV FWHM [9]). The main disadvantage of hypernuclear electroproduction is the very low cross section (of the order of 10 nb/sr^2/GeV), which depends on strongly the kinematical condition and particularly on the electron scattering angle. In summary, information from all of these reactions can allow a complete investigation of hypernuclear states and can provide valuable information on the Λ-N interaction and on the many body hadronic systems due to the use a new degree of freedom: the strangeness.

The E94-107 experiment performed in Hall A at JLab [10] has started a systematic study of hypernuclei formed by several target nuclei in the 1p shell region, such as ^{9}Be, ^{12}C, and ^{16}O. Here the preliminary results of the ^{9}Be$(e,e'\ K)^{9}_{\Lambda}$Li and ^{16}O$(e,e'K)^{16}_{\Lambda}$N reactions are presented.

The JLab Hall A is particularly suited to this task for several reasons. The disadvantage of the small electromagnetic cross section is partially compensated by the high electron current (100 μA), the high duty cycle, and high resolution of the electron beam. Kinematics were set to detect both electrons and kaons at 6 degree with respect to the incident beam with an energy of 3.77 GeV. The registered scattered electrons and final kaons have momentum of 1.86 GeV/c and 1.99 GeV/c, respectively. The virtual photons have energy of 2.2 GeV and momentum squared of $-Q^2$ = -0.079 (GeV/c)^2. Under these conditions, the counting rate is reasonable high since it strongly depends on the Q^2 via the virtual photon flux. The smaller the scattered angles, the smaller the Q^2 and, consequently, the higher the virtual photon flux. At the same time, to keep a reasonable kaon survival fraction, the kaon momentum must be relatively high. A waterfall target 120 mg/cm^2 thick and a solid BeO layer 149 mg/cm^2 thick have been used.

2 Experimental set-up

The standard equipment of Hall A is composed by two high resolution spectrometers (HRS) for the scattered electron and the produced hadron [11]. The right arm at the right side of the beam detects electrons, while coincident kaons, or other hadrons like pions and protons, are detected in the left arm. The minimal angular separation between each HRS and the electron beam is 12 degree. To allow the detection of particles at smaller forward angles, 6 degree in our case, a superconducting septum magnet was added to each spectrometer. To allocate the septa, the scattering chamber was moved 80 cm upstream. The septa, while preserving the HRS optical performances, especially the missing mass (or energy) resolution, produce a small decrease of their angular acceptance (from 6 to 4.5 msr). A detailed description of the septum magnets and of their performances with respect to the standard Hall A configuration is illustrated in reference [12].

A quite unique device, used in the experiment on ^{16}O, is the waterfall target system. The conceptual design of the waterfall target system for Hall A is very similar to the one used at Saclay [13]. The thickness of the waterfall target can be modulated by changing the pump speed; this adds flexibility to the system and allows the user to choose the best value according to the wanted resolution and luminosity. The water, continuously pumped from a reservoir, goes through a heat exchanger into the target zone, and then back into the reservoir. All parts in contact with the water are made of stainless steel. In the target zone, the water pressed through a system of slits and holes and guided by the stainless steel bars forms one or more flat rectangular films, which are stable due to the surface tension and to the adherence to the guiding bars. The entrance and exit windows of the target cell are circular (40 mm in diameter) and are made of gold-plated Be (75 μm thick). Scattered particles go through the 'lateral' windows, made of stainless steel (25 μm thick, dimension of 320×8 mm^2).

The energy resolution of produced hypernuclear spectra depends on three factors: the momentum resolution of the spectrometers, the straggling and energy loss of particles in the target, and the beam energy spread. The momentum resolution of the systems (HRS + septum) is $\Delta p/p = 10^{-4}$ (FWHM). The energy beam spread was as small as 6×10^{-5}, and the target sample mass is so light that straggling can be neglected. All these factors provided a very good energy resolution, of the order of 650 keV FWHM, in the first ${}^{12}_{\Lambda}$B hypernuclear spectrum investigated from the E94-107 collaboration.

A good particle identification system (PID) both in the electron, and, mainly, in the hadron arm, is mandatory in this experiment. A strong pion contamination is present in the electron arm. The use of the Gas Cherenkov counters reduces the electron to pion ratio to 1.3, while a stronger reduction of two order of magnitude is obtained by the lead glass shower counters. The total pion rejection ratio is 10^{-4}. In the hadron arm, the standard PID is obtained by two Aerogel Cherenkov counters (A1, A2) with different refractive index (n_{A1}=1.015 and n_{A2}=1.055), and by the time-of-flight (TOF) between the two HRSs. A 2 GeV/c momentum pion fires both aerogels, while kaon emits Cherenkov light only in A2. Instead protons are below the Cherenkov threshold both in A1 and in A2. Hence an appropriate logic between the two Cherenkov counters should be able to supply a sufficient particle identification (PID). However, possible inefficiencies are introduced by δ-rays from electron or pion. Moreover, identified kaons are contaminated by pions and protons, produced more copiously in our reaction. In these conditions the signal to noise ratio would be unacceptable for the missing mass spectra and would bring to a lack of physical information.

In order to improve the PID and to reduce the background component, a Ring Imaging CHerenkov (RICH) counter has been built and installed in the focal plane of the hadron HRS. The RICH uses a proximity focusing configuration, a C_6F_{14} gas radiator and a CsI photocatode coupled to a Multiwire Parallel Chamber. Its design is identical to the ALICE RICH [14]. More details on the RICH and on its performances are reported in another contribution to this conference [12].

3 Preliminary results

The raw missing mass spectrum on the waterfall is drawn in Figure 1. This spectrum is obtained detecting in coincidence the scattered electron and the produced kaon. Electrons are identified by a two-dimensional selection on the Shower versus PreShower plot and by an additional condition to the Gas-Cherenkov counter. In this way δ-rays induced by pion collisions are eliminated. In the hadron arm, the kaon selection is obtained combining cuts on the two Aerogel counters (A1 and A2), the TOF and the RICH selections. In addition, only particles which produce only one track in the Vertical Drift Chamber (VDC) are considered. The detection efficiencies of all detectors and the electronic dead-time are estimated run by run for the different kinds of events (triggers). In order to perform a

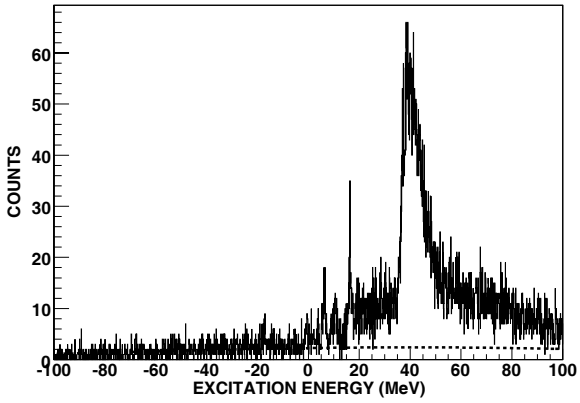

Fig. 1. Missing mass spectrum of the waterfall target as a function of the excitation energy. The dashed line represents the background level. Its low value indicates the good signal to noise ratio achieved in the experiment.

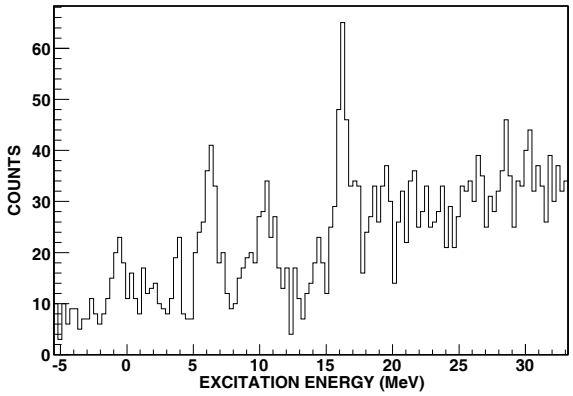

Fig. 2. The ${}^{16}_{\Lambda}$N Spectrum of hypernucleus as obtained after the background subtraction.

comprehensive check of the run quality, the ratio between the number of detected pions over the electric charge delivered by the accelerator is monitored continuosly. Pions are well identified in our experiments and are produced copiously. Thus that ratio can easily evidence eventual failures of the many complex systems of the experiment, like triggers, electronics, detectors, targets, beam, and data acquisition. That ratio is constant within few percents for good data, whereas it strongly deviates for runs with failures.

The dashed line in Figure 1 shows the fitted background. Its low value evidences the good kaon identification obtained in the experiment. The background subtracted spectrum of ${}^{16}_{\Lambda}$N, reported in Figure 2, shows peaks with a FWHM of 1.2 MeV. This resolution is worse than that obtained in the case of a ^{12}C target. A preliminary estimation of the five-folded differential cross section in the laboratory frame indicates that for the ground state it amounts to 1.2 nbarn/sr^2/GeV, which is by 30% lower than theoretical estimations [10].

The hypernucleus formed from the Be target shows a complex structure. Its background subtracted missing mass spectrum, is shown in Figure 3. The level density of the ${}^{9}_{\Lambda}$Li is higher than that of the ${}^{16}_{\Lambda}$N. Two or more

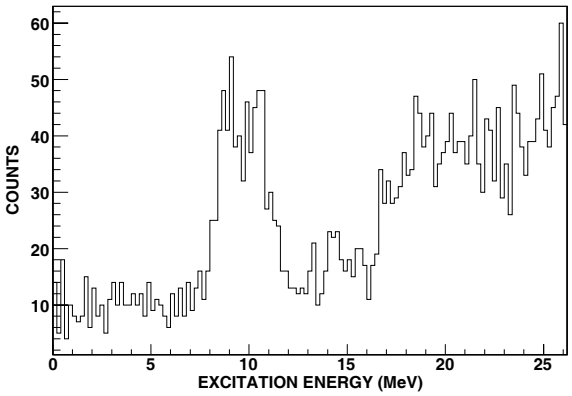

Fig. 3. The ${}^{9}_{\Lambda}$Be hypernuclear spectrum as obtained after the background subtraction.

doublets can be grouped in the main peak. The average level spacing theoretically estimated for this hypernucleus is around 600 keV [10]. The reaction cross section is lower with respect to the hypernuclear electroproduction on the ^{12}C and ^{16}O. In those conditions more work is necessary to separate the levels in clean way in order to extract useful information.

4 Conclusion

The preliminary spectra of the ${}^{9}_{\Lambda}$Li and ${}^{16}_{\Lambda}$N hypernuclei, measured in Hall A at JLab, have been presented in this communication. Missing mass spectra with high signal to noise ratio have been obtained. The hypernuclear spectra show a good energy resolution of nearly 1.2 MeV FWHM which however is not sufficient to separate the several spin-doublet states of these hypernuclei. Further analysis work is underway to obtain the definitive spectra and for their comparison with theoretical predictions.

References

1. J. LeRose *et al.*, these proceedings and references therein.
2. O. Hashimoto *et al.*, these proceedings and references therein.
3. T. Miyoshi *et al.*, Phys. Rev. Lett. **90**, (2003) 232502.
4. L. Yuan *et al.*, Phys. Rev. C **73**, (2006) 044607.
5. R. Chrien *et al.*, Phys. Lett. B **89**, (1979) 31.
6. T. Hasehawa *et al.*, Phys. Rev. Lett. **74**, (1995) 224.
7. M. Agnello *et al.*, Phys. Lett. B **622**, (2006) 35.
8. O. Hashimoto, H. Tamura, Prog. Part. Nucl. Phys. **57**, (2006) 564.
9. M. Iodice *et al.*, in preparation to Phys. Rev. Lett.
10. F. Garibaldi *et al.*, *High Resolution 1p shell Hypernuclear Spectroscopy*, Proposal to JLab (1994).
11. M. Alcorn *et al.*, Nucl. Instrum. Methods A **522**, (2004) 294.
12. F. Cusanno *et al.*, these proceedings and references therein.
13. F. Garibaldi *et al.* Nucl. Instrum. Methods A **314**, (1992) 1.
14. ALICE Collaboration, HMPID TDR, CERN/LHCC98-19, 14 August 1998.